Spawning origins and ontogenetic movements for demersal fishes: An approach using eye-lens stable isotopes

Julie L. Vecchio and Ernst B. Peebles

SEDAR74-RD89

August 2021

This information is distributed solely for the purpose of pre-dissemination peer review. It does not represent and should not be construed to represent any agency determination or policy.

Estuarine, Coastal and Shelf Science 246 (2020) 107047

Contents lists available at ScienceDirect

Estuarine, Coastal and Shelf Science

journal homepage: http://www.elsevier.com/locate/ecss

Spawning origins and ontogenetic movements for demersal fishes: An approach using eye-lens stable isotopes

Julie L. Vecchio [b], [*], Ernst B. Peebles [a]

[a] College of Marine Science University of South Florida, St. Petersburg, FL, 33701, USA
[b] Fish and Wildlife Research Institute, Florida Fish and Wildlife Conservation Commission, 100 8th Avenue SE, St. Petersburg, FL 33701, USA

ARTICLE INFO

Keywords:
Stable isotope analysis
Ontogeny
Larval movement
Grouper
Snapper
USA
Eastern Gulf of Mexico

ABSTRACT

The larval to postlarval period (the period between egg and juvenile) of many continental-shelf fish species lasts only a few weeks but has been shown to be critical to survival. During this period, individuals may travel long distances from spawning to juvenile habitats and are often difficult to locate. Fish eye lenses, which are constructed sequentially with minimal tissue turnover, record successive isotopic values for the entire lifespan. We present a widely applicable method of using the isotope values from the inner-most eye lens lamina (core: representing the larval to postlarval period) as a historical record of early life movement and location. By correlating the eye-lens core δ^{13}C and δ^{15}N values with juvenile capture location (i.e. settlement habitat) or with core size (i.e., growth during the first few weeks of life), we interpreted variability within the isotope values of a species as geographic origin and movement. We then evaluated the method using four northeastern Gulf of Mexico reef-fish species. Gag isotope values indicated movement inshore during the postlarval period. Red Grouper values suggested movement in both the inshore and alongshore directions. Black Seabass isotope values indicated a widely distributed early life with potential southward movement. Red Snapper isotope values suggested that larvae and postlarvae are widely distributed along the outer continental shelf, but do not move far from spawning origins in the eastern Gulf of Mexico. Bulk isotope values in fish eye lens cores can strengthen early life origin and movement data for many species of marine fishes, including those for which little early-life information exists.

1. Introduction

Many continental shelf fish species use disparate habitats throughout life (e.g., Kurth et al., 2019; Coleman and Williams, 2002; Hanson et al., 2013), with spawning occurring far from juvenile settlement locations (Saul et al., 2012; Weisberg et al., 2014; Tzadik et al., 2015). Whereas the larval to postlarval period (the period between egg and juvenile) lasts only weeks in most bony fishes, it can be critical in the survival of individuals and populations in many marine species (Houde, 2009). Because planktonic or semi-planktonic fish larvae can drift extensive distances, larval collections of coastal fish species are often spatially decoupled from both spawning and juvenile habitats (Colin, 2012; Burghart et al., 2014; Weisberg et al., 2014). Moreover, the larvae collected in ichthyoplankton surveys may not represent the proportion of the population that survives to the juvenile or adult stage (Burghart et al., 2014).

Bulk stable isotope values can be used as natural tags, providing information on geographic location (Seminoff et al., 2012; Trueman et al., 2017), movement (McMahon et al., 2011; MacKenzie et al., 2012), and trophic position (Post, 2002; Guinan et al., 2015; Dalponti et al., 2018). Many isotope-based investigations have focused on white muscle or other rapidly regenerating tissues (e.g. Brame et al., 2014; Haas et al., 2009; McMahon et al., 2013). Archival tissues such as otoliths (Dorval et al., 2007) and eye-lenses (Tzadik et al., 2017) have the potential to provide isotopic histories, including movement during the larval period (Nishida et al., 2020).

Fish eye lenses grow throughout life, sequentially adding thin layers of cells (laminae) to the outer margin of the lens (Nicol, 1989; Vihtelic, 2008). As lens size increases, the amount of protein required to cover the outside of the lens also increases. Because new lens cells experience minimal reworking after formation, the bulk isotopic composition of each eye-lens lamina reflects isotopic composition within the body

---

[*] Corresponding author. Fish and Wildlife Research Institute, Florida Fish and Wildlife Conservation Commission, 100 8th Avenue SE, St. Petersburg, FL 33701, USA.

E-mail address: jvecchio@usf.edu (J.L. Vecchio).

https://doi.org/10.1016/j.ecss.2020.107047
Received 4 June 2020; Received in revised form 17 September 2020; Accepted 29 September 2020
Available online 3 October 2020
0272-7714/© 2020 Elsevier Ltd. All rights reserved.

during the time of lamina formation (Lynnerup et al., 2008; Nielsen et al., 2016). Thus, fish eye lenses sequentially preserve lifetime bulk stable isotope records (Wallace et al., 2014; Quaeck-Davies et al., 2018; Curtis et al., 2020) that can be reconstructed with an approximate frequency of two to three months (Wallace et al., 2014; Granneman, 2018). Some marine fishes, such as sharks and rays, rely on maternal nutrition for extended periods during early life, which is reflected in the isotope values of the eye-lens (Simpson et al., 2019). However, most marine bony fishes begin exogenous feeding within 72 h of hatching and at a total body length of only a few mm (Mullaney and Gale, 1996; Berlinsky et al., 2000; Drass et al., 2000; Lim and Mukai, 2014). Thus, the δ^{13}C and δ^{15}N values of the inner-most eye-lens material (hereafter, the eye-lens "core") reflect the geographic location and diet (trophic position and basal-resource dependence) during the earliest weeks of life in these species (Wallace et al., 2014; Curtis et al., 2020).

The West Florida Shelf (WFS) in the northeastern Gulf of Mexico is a mosaic of soft- and hard-bottom habitats (Locker et al., 2010; Hine and Locker, 2011; Wall and Stallings, 2018) that extend over 600 km from north to south and over 200 km west from the Florida peninsula. Background isotope values and ranges in this region (Fig. 1a) remain remarkably stable among species, seasons, and years (Radabaugh et al., 2013; Huelster, 2015; Peebles and Hollander, 2020). The total range of background δ^{15}N values for the region is approximately 4.4‰ (Fig. 1a) with variation in δ^{15}N values likely driven by spatial variation in fluvial input and nitrogen fixation. Values of δ^{15}N are highest toward the northwestern WFS and lowest to the southeast, coinciding with distance from large freshwater inflows that contribute terrestrial nitrogen to the north-central Gulf of Mexico (Radabaugh and Peebles, 2014; Peebles and Hollander, 2020). The total range of background δ^{13}C values is approximately 3.6‰ (Fig. 1a). Trends in background δ^{13}C values are roughly orthogonal to δ^{15}N, with δ^{13}C values highest close to shore and lowest close to the shelf edge. These trends are likely driven by photosynthetic fractionation, microalgal species composition, and/or changes in reliance on benthic or planktonic microalgae as basal resources (Radabaugh et al., 2014). Light environment, in particular, is thought to influence photosynthetic fractionation with shallow, clear water resulting in higher baseline δ^{13}C values (less fractionation) than deep, less-clear waters (Fry and Wainright, 1991; Radabaugh et al., 2014). The primary trends in water depth and water clarity as well as location and relative volume of fluvial input tend to be stable on the WFS over time, resulting in stable background δ^{13}C and δ^{15}N values for the region.

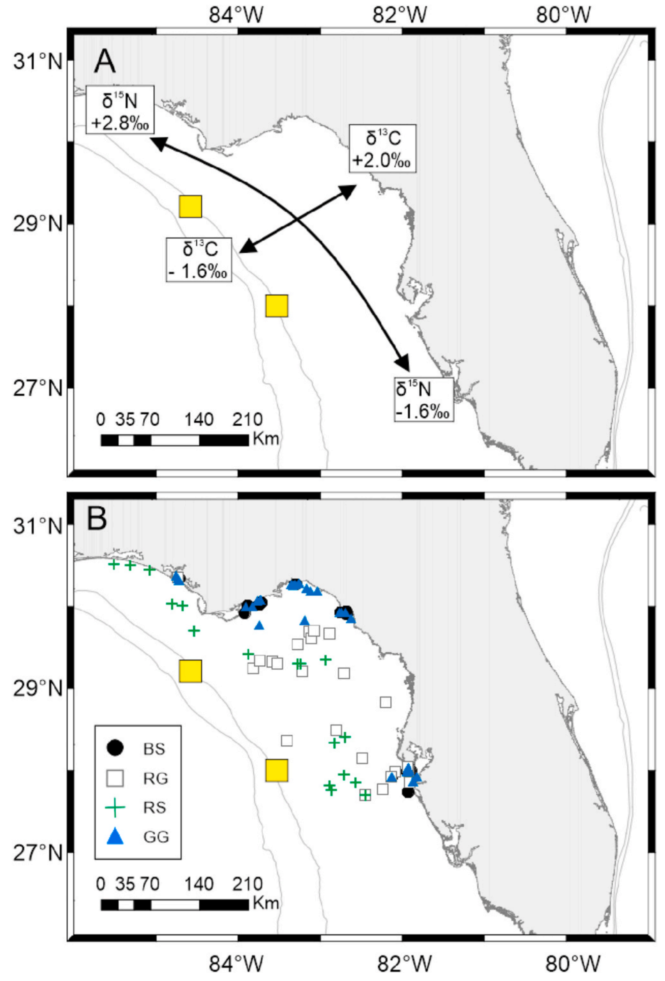

Fig. 1. Region of interest, northeastern Gulf of Mexico. Bathymetry lines represent 100 m and 200 m depth contours. Yellow boxes indicate approximate locations of marine protected areas designed to maintain grouper and snapper spawning habitat. A. Deviation from mean background δ^{15}N and δ^{13}C values based on (Radabaugh and Peebles, 2014) and (Peebles and Hollander, 2020). Numbers represent the range of values, not absolute values of either isotope, in fish tissue. B. Capture locations for juveniles of the four species examine. Black Seabass (BS), Red Grouper (RG), Red Snapper (RS), and Gag (GG).

Many commercially and recreationally valuable fish species use the WFS throughout their lifespans, yet the larval and postlarval periods remain largely unstudied in many species due to complex life histories, difficulty accessing specimens, and a large geographic region. Red Grouper (*Epinephelus morio*) inhabit low-relief, hard-bottom areas of the WFS, with juveniles occurring in shallower water than adults (Moe, 1969; Johnson and Collins, 1994; Lombardi-Carlson, 2014). This species has been observed spawning in small groups scattered across the WFS (Coleman et al., 1996, 2010), with the highest spawning activity recorded near the 70 m isobath (Wall et al., 2011; Grasty et al., 2019). Gag (*Mycteroperca microlepis*) spawn in large groups near the outer WFS (Fitzhugh et al., 2005; Ellis and Powers, 2012). Juvenile Gag subsequently inhabit the polyhaline regions of embayments for a year or more (Stallings et al., 2010; Switzer et al., 2012), and non-spawning adults use high-relief habitats in the shallow coastal zone (Bullock and Smith, 1991). Black Seabass (*Centropristis striata*) tend to be concentrated in low-relief, hard-bottom regions of the northern WFS (Hood et al., 1994; Weaver, 1996), with little data available to indicate whether ontogenetic habitat shifts occur. Red Snapper (*Lutjanus campechanus*) have recently re-expanded their range southeastward along the WFS after several years of strict harvest controls (Hollenbeck et al., 2015). Planktonic Red Snapper eggs have been genetically identified, and several females with hydrated oocytes have been captured on WFS reefs (Burrows et al., 2018; Nguyen, 2020), indicating spawning now occurs in the region. However, the distributions of spawning locations, eggs, and larvae on the WFS are unknown.

The objective of this study was to create a broadly applicable interpretation method for inferring fish early-life geographic origins and movement patterns using eye-lens stable isotope data. We used simultaneous correlation (Du et al., 2003; Zhang et al., 2006; Mahmoud and Sunarso, 2018) to evaluate the geographic origins and movements of demersal species from the northeastern Gulf of Mexico. Two of the species (Red Grouper and Gag) had well-known spawning and juvenile locations while these parameters were less well-understood in the other two (Red Snapper and Black Seabass). The current work represents a test case, but we designed the approach to be applicable to the study of any fish species in any region with consistent background isoscape trends.

2. Materials and methods

2.1. Specimen collection

We obtained juvenile Black Seabass (n = 51), Gag (n = 51), Red Grouper (n = 52), and Red Snapper (n = 38) from the fisheries-independent monitoring efforts of the Florida Fish and Wildlife Conservation Commission and the Southeast Area Monitoring and

Assessment Program (SEAMAP). Between 2015 and 2017, specimens were collected from the WFS and from the mouths of embayments on the west coast of Florida (Fig. 1b). We measured each fish for standard length (SL). We extracted both eyes, wrapped them in aluminum foil, and froze them at -20 °C until analysis. We extracted, dried, and cleaned otoliths from each fish. Aging was completed by counting annuli using a dissecting stereomicroscope and transmitted light. Black Seabass, Gag, and Red Grouper otoliths were aged whole (Casselman, 1990; Kimura and Lyons, 1991). Red Snapper otoliths were thin sectioned using an IsoMet low-speed saw and mounted on a slide before aging (White and Palmer, 2004).

2.2. Eye lens preparation and sample analysis

We thawed one eye from each fish and removed the lens. We separated (delaminated) eye-lens laminae using two sets of fine-tipped forceps under a dissecting stereomicroscope. We followed the methods of Wallace et al. (2014), but immersed each lens in deionized water for delamination (Stewart et al., 2013; Meath et al., 2019), changing the water each time a lamina was removed. Only the innermost tissue (eye-lens core) was used for this analysis. The core was operationally defined as the smallest sphere of tissue at the center of the eye lens that could be manually isolated while retaining sufficient mass for isotope analysis. We measured the eye-lens core diameter (ELD) to the nearest 0.05 mm using a calibrated ocular micrometer; the cores ranged in diameter from 0.3 to 1.1 mm (Table 1). In some fish, a single core did not provide sufficient mass for isotopic analysis (minimum mass = 150 μg, unpublished data), in which case we obtained the equivalent-sized core from the second eye lens of the same fish and combined the two cores (Peebles and Hollander, 2020). Left and right eye lens laminae from the same individual have been shown to provide nearly identical isotope values at similar diameters (Wallace et al., 2014). If delaminated diameters were not within the unit of measurement (0.05 μm), we discarded both cores and the specimen was eliminated from analysis. We placed all core samples in a drying oven at 55 °C for 12 h to ensure complete desiccation.

We packaged eye-lens core samples with a mass of 150–600 μg into 3.3 × 5 mm tin capsules and used a Carlo-Erba NA2500 Series II elemental analyzer coupled to a continuous-flow Thermo-Finnigan Delta + XL isotope ratio mass spectrometer (IRMS) at the University of South Florida College of Marine Science in St. Petersburg, Florida, for all isotope analyses. Calibration standards were NIST 8573 and NIST 8574 L-glutamic acid standard reference materials. Analytical precision, obtained by replicate measurements of NIST 1577b bovine liver, was ±0.20‰ for δ^{13}C and ±0.17‰ for δ^{15}N (n = 200 replicates). Results are presented in standard notation (per mil notation, ‰) relative to the international standards air and Vienna Pee Dee Belemnite,

$$\delta X = \left(\frac{R_{sample}}{R_{standard}} - 1\right) \times 1000$$

where X is the element (carbon or nitrogen) and R is the corresponding ratio ^{13}C/^{12}C or ^{15}N/^{14}N.

2.3. Data analysis methods

We completed all statistical analyses in R version 3.6.1 (R Core Team, 2019). We constructed species-specific best-fit regression equations for fish standard length (SL) as a function of maximum eye-lens diameter at capture (note that this value is distinct from the core ELD used in all other analyses). We used these regressions to calculate SL for each specimen at the time of eye-lens core completion. We then compared calculated SLs to the published SL at settlement for each species (Table 1) to ensure that each core represented the post-larval/early juvenile period. We also calculated mean and standard error for the eye-lens-core isotope values for each species (Table 1).

We compared the multivariate differences in eye-lens core stable isotope values among species using PERMANOVA [Package vegan; Adonis routine (Oksanen et al., 2019)] and multivariate pairwise comparisons [package EcolUtils (Salazar, 2019);]. We calculated the dispersion of δ^{13}C and δ^{15}N values using stable isotope Bayesian ellipses in R (SIBER), which describes aspects of a population's isotopic dispersion by plotting and measuring the bivariate standard deviation, or standard ellipse area (SEAc), of isotope biplots (Jackson et al., 2011). We considered differences in SEA$_c$ to be significant between species if ≥ 95% of posterior draws for one species was smaller than for the other. We also used SIBER to measure the degree of overlap between isotopic distributions for each species.

We interpreted isotope values as representing the entire period of eye-lens core formation, recognizing that this isotopic information is likely biased toward the latter part of the postlarval/early juvneile period due to proportionally larger masses of lens material added to the lens as the fish grows. We constructed a matrix of theoretical trends (positive, negative, or neutral) that would result from species-wide departures of regression slopes from zero produced by the influences of geographic origin (Lorrain et al., 2015), geographic movement (Acosta-Pachon et al., 2020), and change in trophic position (Wallace et al., 2014) on isotope values. We then provided the potential observed outcomes of combining these various inputs into a single bulk isotope value (Fig. 2).

Similar to the approach of Meath et al. (2019), we used a series of correlations to separate the geographic influences. We considered the geographic movements necessary to produce positive, negative, or no correlation between eye-lens core isotope values and three independent

Table 1
Capture information and regression parameters used to convert eye-lens diameters to fish length at eye-lens core formation. For each of the four species number collected, collection length, collection age, and size of analyzed eye-lens core (ELD), mean (±SE) values of both δ^{13}C and δ^{15}N are listed. Regression equation used to calculate standard length (SL), R^2, slope p-value and estimated SL at analysis. Additional information on SL (mm) and age (d) at metamorphosis from postlarva to juvenile are provided from literature.

	Black Seabass	Gag	Red Grouper	Red Snapper
Number specimens	51	52	51	38
Collection SL (mm)	48–231	94–321	37–256	140–325
Collection age (yr)	0–3	0–2	0–2	1–3
ELD (mm)	0.4–1.1	0.3–0.8	0.4-1.0	0.4-0.8
Mean δ^{13}C ± SE	−18.49 ± 0.20	−19.02 ± 0.16	−19.26 ± 0.12	−18.96 ± 0.14
Mean δ^{15}N ± SE	8.12 ± 0.20	7.33 ± 0.11	7.05 ± 0.09	7.97 ± 0.24
Regression equation	SL = 35.33*ELD	SL = 56.54*ELD	$SL = (5.94*\sqrt{(ELD)})^2$	$SL = (6.02*\sqrt{(ELD)})^2$
Est. SL at analysis (mm)	15–40	18–47	14–36	15–29
Slope p-value	<0.001	<0.001	<0.001	<0.001
R^2	0.98	0.96	0.99	0.99
Metamorphosis SL (mm)	11	17–25	20	21
Metamorphosis age (d)	20–35	29–52	35	30–35
Source (Metamorphosis)	Roberts et al. (1976)	Fitzhugh et al. (2005)	Colin et al. (1996)	Drass et al. (2000)

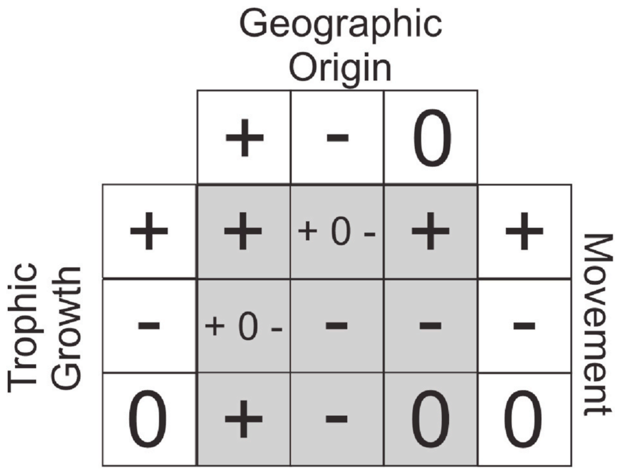
Geographic Origin
+
-
0
Trophic Growth
+
-
0
Movement
+
-
0
+
+ 0 -
+
+ 0 -
-
-
+
-
0

Fig. 2. Expected isotopic outcomes (gray cells: increase, decrease, or no change) of all possible combinations of three effects (white cells): geographic origin (the geographic distribution of spawning), trophic growth (changes in trophic position over the time period represented by the samples), and movement along an isotopic gradient over the same period. Species-level trends can be positive, neutral, or negative (+, 0, -). Mixed inputs can result in variable outcomes.

parameters: ELD (proxy for body size), capture latitude, and capture longitude (known juvenile habitat; Fig. 3, Table S1). We used Spearman rank correlations to lessen sensitivity to small sample sizes, non-normal distributions, and extreme outliers (Sokal and Rohlf, 1994). All data are published in the Gulf of Mexico Research Initiative Information and Data Cooperative (GRIIDC) website (https://data.gulfresearchinitiative.org/data/R1.x135.120:0012).

3. Results

Age at collection ranged from under one year to over three years, and collection length ranged from 37 to 325 mm SL. Based on species-specific regressions between ELD and SL, the analyzed fish were in the range of 14–47 mm SL at the time of outer core formation, ranging from a few days pre-settlement (postlarval) to a few weeks post-settlement (early juvenile: Table 1). Mean values of both δ^{13}C and δ^{15}N were highest for Black Seabass with wide ranges in both. Red Snapper produced the largest range of δ^{15}N values and a small range of δ^{13}C values. Gag and Red Grouper isotope values were both lower and total ranges smaller in both directions than for the other two species (Fig. 4).

3.1. Statistical differences among species

We found significant multivariate differences among the core isotope values of the four species (PERMANOVA F = 8.42, $p < 0.001$). Black Seabass and Red Snapper were each significantly different from Red

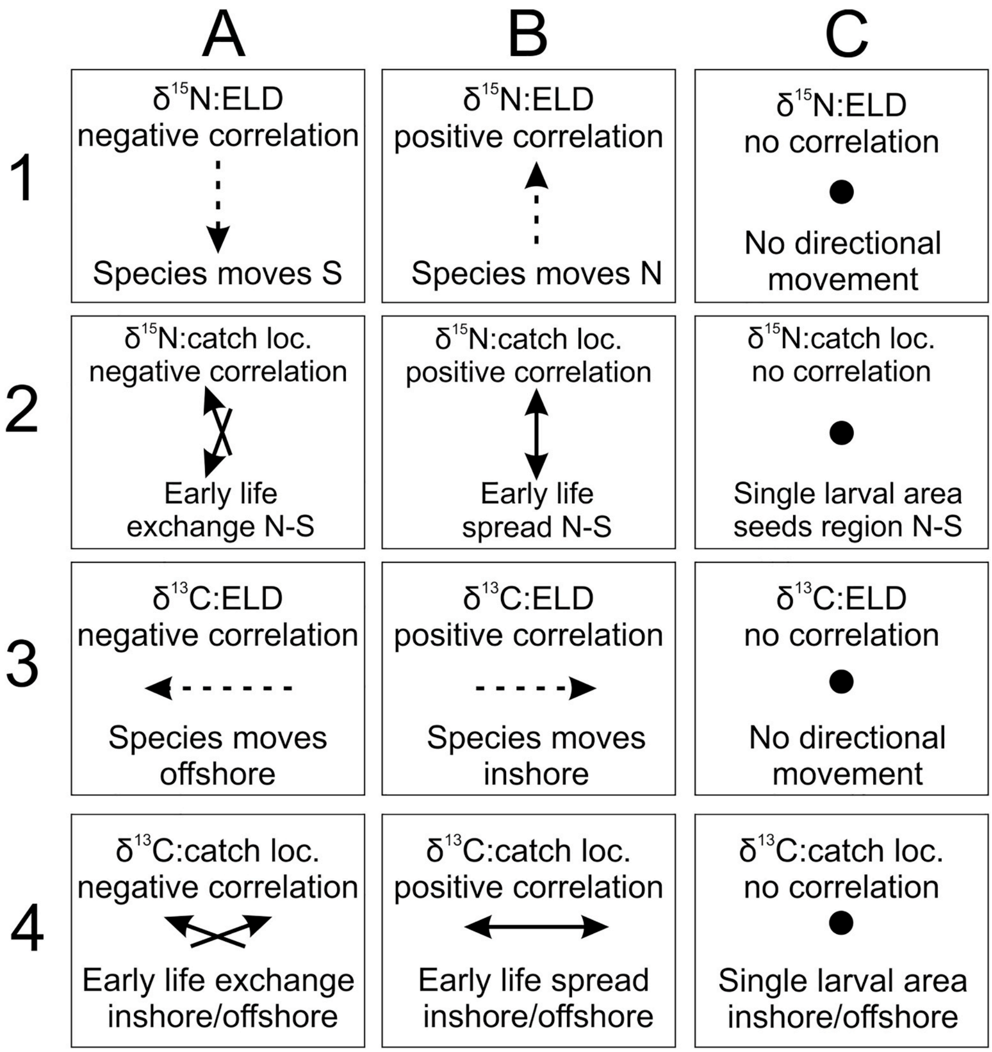
A
B
C
1
δ15N:ELD negative correlation
Species moves S
δ15N:ELD positive correlation
Species moves N
δ15N:ELD no correlation
No directional movement
2
δ15N:catch loc. negative correlation
Early life exchange N-S
δ15N:catch loc. positive correlation
Early life spread N-S
δ15N:catch loc. no correlation
Single larval area seeds region N-S
3
δ13C:ELD negative correlation
Species moves offshore
δ13C:ELD positive correlation
Species moves inshore
δ13C:ELD no correlation
No directional movement
4
δ13C:catch loc. negative correlation
Early life exchange inshore/offshore
δ13C:catch loc. positive correlation
Early life spread inshore/offshore
δ13C:catch loc. no correlation
Single larval area inshore/offshore

Fig. 3. Interpretations of all possible correlations between eye lens isotope value (δ^{13}C or δ^{15}N) and fish size expressed as eye-lens diameter (ELD) or known catch latitude or longitude (loc.) at species level. Significant correlations between isotope value and ELD indicates fish move in a particular direction (N = north, S = south) along known isotopic trends during the larval/postlarval period; non-significant correlation indicates no such movement. Significant correlation between isotope value and catch location suggests juveniles found in different habitats originated from different regions. Non-significant correlations indicate juvenile in several locations come from a single source population. (Interpretations for each species are presented in Table 3 with additional description provided in Table S1).

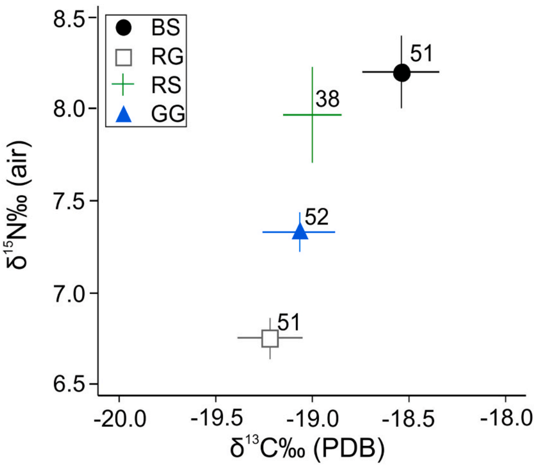

Fig. 4. Mean (±SE) eye-lens core δ^{13}C and δ^{15}N values by species (‰) and number of samples per species for Black Seabass (BS), Gag (GG), Red Grouper (RG), and Red Snapper (RS).

Table 2
Pairwise SEAc proportion overlap and PERMANOVA comparisons (global PERMANOVA: F = 8.42, p < 0.001). Proportional overlap between SEAc are not evaluated for significance. Adjusted *p*-values for pairwise PERMANOVA are presented as not significant (n.s.), * < 0.05, ** < 0.01, *** < 0.001. Global PERMANOVA (F = 8.42, *p* < 0.001).

SEAc proportional overlap (%)			
	Black Seabass	Gag	Red Grouper
Gag	21		
Red Grouper	8	49	
Red Snapper	48	43	26
PERMANOVA Pairwise Comparisons			
	Black Seabass	Gag	Red Grouper
Gag	0.072 **		
Red Grouper	0.149 ***	0.026 (n.s.)	
Red Snapper	0.017 (n.s.)	0.042 *	0.115 **

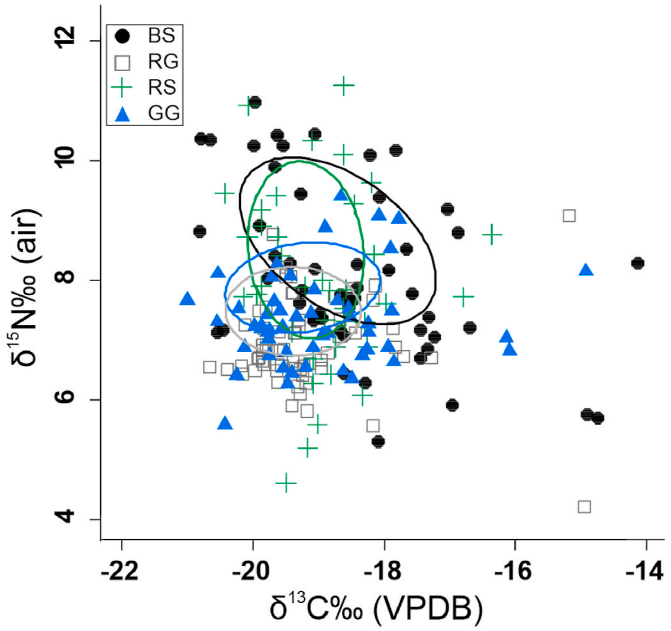

Fig. 5. Eye-lens core δ^{13}C and δ^{15}N values by species. Each data point represents the δ^{15}N and δ^{13}C values for the core eye-lens from an individual fish. Superimposed on the scatterplot are standard ellipses containing 40% of the observations for each species (from SIBER routine in R). Species are Black Seabass (BS), Gag (GG), Red Grouper (RG), and Red Snapper (RS).

Grouper and from Gag (Table 2). SEAc was largest for Black Seabass (5.83 ± 1.52‰^{2}) and smallest for Red Grouper (2.40 ± 0.59‰^{2}); Red Snapper (4.13 ± 1.27‰^{2}) and Gag (2.77 ± 0.74‰^{2}) were intermediate. Black Seabass SEAc extent was significantly larger than both Gag and Red Grouper but not significantly different from Red Snapper (Fig. 5). Overlap in SEAc between species ranged from 8 to 49% (Table 2).

3.2. Isotopic correlations with body size and juvenile habitat location

For Black Seabass, correlations between location (latitude or longitude) and isotope values (both δ^{15}N and δ^{13}C) were significant. However, only δ^{15}N values correlated significantly with ELD. For Gag, δ^{13}C values correlated with ELD while δ^{15}N values correlated with latitude. For Red Grouper, both δ^{13}C and δ^{15}N values correlated with ELD, but neither correlated with collection latitude or longitude. In Red Snapper, only δ^{15}N values and latitude correlated (Table 3). Interpretations of the origin and movement patterns for each species indicate differences in both parameters among species (Table 3, Fig. 6). Geographic locations presented are approximate and are positioned according to absolute isotopic differences relative to the known spawning grounds for Gag (i.e., MPAs in Fig. 6). Black Seabass appears to have been the most widely distributed, with a possible, subtle southward movement trend along the WFS. The central area for Red Grouper was the smallest and farthest south and offshore of the four species, with likely movement to the north and inshore. Gag origin area was also relatively small, with substantial inshore movement over the postlarval period. Red Snapper origins were

Table 3
Spearman rank correlations between δ^{15}N value and ELD or collection latitude (lat) and between δ^{13}C value and ELD or collection longitude (lon) by species; *p*-value significance is indicated as n.s. > 0.05 * <0.05, ** <0.01, *** <0.001. Isotopic interpretations refer to those conceptualized in Fig. 3 and Table S1.

Species	δ^{15}N: ELD	δ^{15}N: lat	δ^{13}C : ELD	δ^{13}C : lon	Isotopic Interpretations
Black Seabass	−0.30 *	0.37 **	0.27 (n. s.)	−0.37 **	1A, 2B, 3C, 4A
Gag	−0.02 (n.s)	0.30 *	0.48 ***	−0.10 (n.s.)	1C, 2B, 3B, 4C
Red Grouper	0.54 ***	−0.12 (n.s.)	0.30 *	0.15 (n.s.)	1B, 2C, 3B, 4C
Red Snapper	0.25 (n.s.)	0.63 ***	0.06 (n.s.)	−0.31 (n.s.)	1C, 2B, 3C, 4C

confined in the inshore-offshore direction but were diffuse in the north-south direction. Unlike the other three species, no larval to postlarval movement was detected for Red Snapper.

4. Discussion

We devised a novel strategy for inferring fish spawning distribution and early-life movement using δ^{13}C and δ^{15}N values from eye-lens cores, using known capture locations to aid interpretation. We evaluated the approach using four reef-associated fish species common to hard-bottom habitats of the WFS and found differences in both apparent spawning origin and apparent ontogenetic movement among species. Each species exhibited a unique distribution in both δ^{13}C and δ^{15}N values, suggesting differences in early life distribution and movement. The approach developed here can be adapted for use in other fish species on the WFS and for fish in other geographic regions that have strong trends within isotopic backgrounds (isoscapes).

Bulk δ^{13}C and δ^{15}N values incorporate both trophic position and geographic location into a single value (Graham et al., 2007, 2010; McMahon and McCarthy, 2016). We considered three major influences on the bulk isotopic values within fish eye-lens cores: geographic origin (Trueman et al., 2017), trophic growth (Dalponti et al., 2018; McMeans et al., 2019), and movement along the isotopic gradient (Graham et al., 2010, Fig. 2). The δ^{15}N values in the eye-lens cores were uniformly lower than other regions of the eye lens (data not presented), suggesting the fish were at the lowest trophic position of their lives (Collery et al., 2014; Park et al., 2014) in contrast to species with substantial maternal contributions (Simpson et al., 2019). Because of early exogenous feeding (72 h in these species), the influence of the maternal contributions to these eye lens cores (from yolk) is rapidly lost in the mass balance. Postlarvae of the four species consume similar prey (Powell and Tucker, 1992; Berlinsky et al., 2000; Drass et al., 2000; Umezawa et al., 2018), suggesting that differences in eye-lens core isotope values reflected differences in geographic origin and movement rather than differences in trophic position.

Gag are known to spawn in high-relief areas near the outer WFS (Coleman et al., 1996, 2011). Our Gag collections occurred exclusively inside or very near embayments adjacent to the WFS (Fig. 1b), where shallow, clear water imparts high δ^{13}C values (Barnes et al., 2009; Radabaugh and Peebles, 2014; Trueman et al., 2017). However, eye-lens core isotope values were low, aligning closely with whole-body isotope values of freshly-settling Gag in a previous study (Weisberg et al., 2014). Spearman rank correlation results suggest that young Gag move into areas with higher background δ^{13}C values during the first two months of life (Fig. 6). Gag isotopic SEAc was small with low mean δ^{13}C and δ^{15}N values, suggesting most fish originated from a confined spawning area near the southwestern extent of the study region (Fig. 6). A positive correlation between δ^{15}N value and collection latitude suggests those individuals that spent their postlarval periods farther to the north were also collected as juveniles near embayments farther to the north. Physical models suggest that postlarvae may take advantage of bottom currents to arrive at shallow-water locations that are far from offshore spawning origins (Weisberg et al., 2014).

Red Grouper spawn in small harems spread across low-relief areas of the WFS (Coleman et al., 2010, 2011). Juveniles are often found in the northern WFS and near the mouths of embayments throughout the study region (Fig. 1b), whereas spawning seems to be most common south of

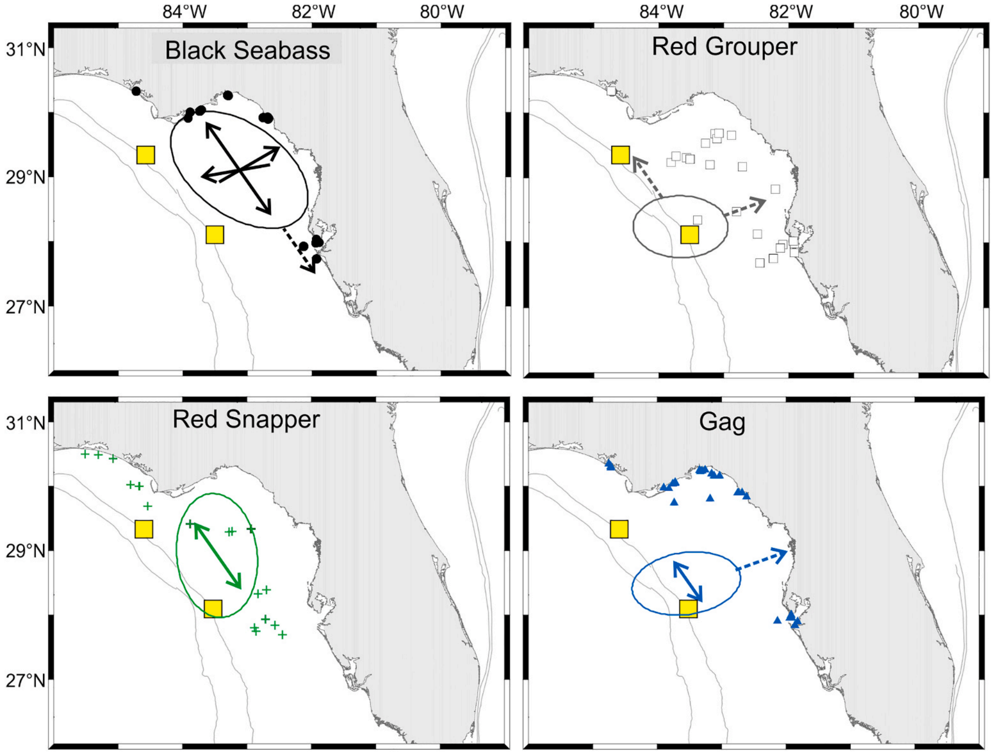

Fig. 6. Schematic representation of early life locations and movement trajectories for larvae/postlarvae of each species based on relationships described in Fig. 3. Yellow squares are Marine Protected Areas. Colored symbols are capture locations of juvenile fish in each species. Ovals represent eye lens core-based early life locations with relative isotopic locations from Fig. 5; the oval for Gag is placed over this species' known spawning grounds, which served as a geo-referencing anchor for the isotopic deviations by the other three species. Solid arrows represent significant relationships between core isotopic values and juvenile capture location (degree of early-life spread). Dashed arrows represent relationship between core isotopic values and eye-lens diameter (ELD; movement during the larval/postlarval period). In both types of arrow, vertical arrow direction represents the known trend in δ^{15}N values for the WFS, with higher values farther northwest. Horizontal arrow direction represents the known trend in δ^{13}C values for the WFS, with higher values closest to the coast.

28°N. Studies inside a marine protected area indicate that Red Grouper reproductive areas are clustered near 70 m depth and persist year after year (Wall et al., 2011; Grasty et al., 2019). Isotopic observations included a wide total δ^{13}C and δ^{15}N value distribution (Fig. 5), which is consistent with scattered spawning areas. The small SEAc for Red Grouper suggests that high densities of spawning occurred in specific subregions of the WFS (Fig. 5). Taken together with the lack of correlation between δ^{15}N or δ^{13}C values and capture location, these data suggest a large proportion of juveniles originated from a confined geographic area well offshore from typical juvenile habitat (Fig. 6).

Adult and juvenile Black Seabass are widely distributed throughout the northern WFS (Hood et al., 1994). However, little is known of their spawning locations or postlarval distribution. In the present study, eye-lens core isotope values were relatively high (Fig. 4) and the standard ellipse areas were large (Fig. 5), suggesting the species originated from a large area of the northern WFS. Significant correlations between the isotope values and collection location indicate settlement distribution was wide in both the along-shelf and inshore-offshore directions (Fig. 6). No correlation between δ^{13}C value and ELD suggests fish were settling near where they were spawned; however, a significant negative correlation between δ^{15}N values and ELD suggests northerly spawning regions may be seeding more southerly populations or groups, which is consistent with wind-driven currents in the region that move water southward throughout much of the year (Mayer et al., 2017).

Red Snapper became rare on the WFS several decades ago, presumably as the result of heavy fishing pressure (Burns and Froeschke, 2012). Recent commercial and recreational catches suggest the species has returned to the central WFS in large numbers, and fishery-independent data indicate spawning is occurring in the region (Burrows et al., 2018; Nguyen, 2020). In the present study, the constrained range of δ^{13}C values and dispersed δ^{15}N values (Table 3; Fig. 6) suggest a narrow depth range but an expansive along-shelf postlarval distribution, increasing confidence that a multi-generational return to WFS habitats is taking place. The lack of correlation between δ^{13}C or δ^{15}N values and ELD suggests no major geographic movement is occurring between the postlarval and juvenile stages, which is consistent with observations from the northern Gulf of Mexico (Wells et al., 2008), indicating Red Snapper are spawning on outer WFS reefs with progeny recruiting to the same general areas.

5. Conclusions and future directions

We show that isotope values within eye-lens cores, combined with juvenile catch location and ELD, yield inferences about spawning location and early life movement that are both consistent with known patterns and are broadly generalizable to populations with less biological information. Differences in the isotopic value central tendencies agreed with known or suspected differences in relative spawning locations and early-life habitat use (Coleman et al., 1996; Weaver, 1996; Saul et al., 2013). We inferred movement during a time window of a few weeks. We added evidence to suggest the recent Red Snapper range expansion involves self-recruitment. While the approach is promising, several future developments could further improve interpretation. First, advances in instrumentation will enable future researchers to use smaller eye-lens samples, potentially further subdividing the available information within the larval/postlarval/early juvenile periods. In addition, compound-specific isotope analysis will increase certainty in the separation between geographic and trophic effects. Finally, isotopic techniques should be paired with other emerging technologies such as ichthyoplankton surveys that identify fish eggs via DNA barcoding (Burrows et al., 2018) to better quantify spawning locations and patterns of movement during early life. With continued development, the current approach can serve as a means of identifying larval and postlarval habitats and movement patterns for less-well-studied species around the world.

Funding

Funding for this research was provided by University of South Florida College of Marine Science endowed fellowships and the Spawning Habitat and Early-Life Linkages to Fisheries (SHELF) project of the Florida RESTORE Act Centers of Excellence Program (FLRACEP), administered by the Florida Institute of Oceanography under awards 4710112604 and 4710112901 to the University of South Florida. These funding sources had no role in the study design, in the collection, analysis and interpretation of data, in the writing of the report, or in the decision to submit the article for publication.

CRediT authorship contribution statement

Julie L. Vecchio: Conceptualization, Data curation, Methodology, Project administration, Visualization, Writing - original draft, Writing - review & editing. **Ernst B. Peebles:** Conceptualization, Data curation, Formal analysis, Funding acquisition, Methodology, Supervision, Visualization, Writing - review & editing.

Declaration of competing interest

The authors declare that they have no known competing financial interests or personal relationships that influenced the work.

Acknowledgements

We thank Florida Fish & Wildlife Conservation Commission's Fisheries Independent Monitoring program and SEAMAP groundfish trawl survey for specimen collections. We thank members of the Peebles lab, especially Catie Bruger, Jennifer Granneman, Brianna Michaud, and Amy Wallace for assistance with dissections and eye-lens preparation. We also thank Ethan Goddard and the USF College of Marine Science Marine Environmental Chemistry Laboratory for isotope analysis. We thank the Fish and Wildlife Reserach Institute Age and Growth Laboratory and Michael Schram for otolith processing and aging. Financial support from JLV included the NOAA/NMFS Marine Resource Assessment fellowship program, the Roche/ARCS fellowship program for college scientists, the Florida Sea Grant Guy Harvey fellowship, the Jack and Katherine Ann Lake fellowship, the Gulf Oceanographic Charitable Trust Fellowship, and the Spawning Habitat and Early-Life Linkages to Fisheries (SHELF) project of the Florida RESTORE Act Centers of Excellence Program (FLRACEP), which is administered by the Florida Institute of Oceanography. This paper is a chapter from JLV's PhD dissertation, which benefitted from input by committee members EBP, Dr. Chris Stallings, Dr. Steve Murawski, Dr. Linda Lombardi, and Dr. Brad Rosenheim.

Appendix A. Supplementary data

Supplementary data to this article can be found online at https://doi.org/10.1016/j.ecss.2020.107047.

References

Acosta-Pachon, T.A., Ortega-García, S., Graham, B., 2020. Assessing residency and movement dynamics of swordfish Xiphias gladius in the Eastern North Pacific Ocean using stable isotope analysis. Mar. Ecol. Prog. Ser. 645, 171–185.

Barnes, C., Jennings, S., Barry, J.T., 2009. Environmental correlates of large-scale spatial variation in the delta C-13 of marine animals. Estuar. Coast Shelf Sci. 81, 368–374.

Berlinsky, D., Watson, M., Nardi, G., Bradley, T.M., 2000. Investigations of selected parameters for growth of larval and juvenile black sea bass Centropristis striata L. J. World Aquacult. Soc. 31, 426–435.

Brame, A.B., McIvor, C.C., Peebles, E.B., Hollander, D.J., 2014. Site fidelity and condition metrics suggest sequential habitat use by juvenile common snook. Mar. Ecol. Prog. Ser. 509, 255–269.

Bullock, L.H., Smith, G.B., 1991. Seabasses (pisces: serranidae). Mem. Hourglass Cruises 8, 1-243.

Burghart, S.E., Van Woudenberg, L., Daniels, C.A., Meyers, S.D., Peebles, E.B., Breitbart, M., 2014. Disparity between planktonic fish egg and larval communities as indicated by DNA barcoding. Mar. Ecol. Prog. Ser. 503, 195–204.

Burns, K.M., Froeschke, J.T., 2012. Survival of Red Grouper (*Epinephalus morio*) and red snapper (*Lutjanus campechanus*) caught on J-hooks and circle hooks in the Florida recreational and recreational-for-hire fisheries. Bull. Mar. Sci. 88, 633–646.

Burrows, M., Browning, J.S., Breitbart, M., Murawski, S.A., Peebles, E.B., 2018. DNA barcoding reveals clear delineation between spawning sites for neritic versus oceanic fishes in the Gulf of Mexico. Fish. Oceanogr. 1–12.

Casselman, J.M., 1990. Growth and relative size of calcified structures of fish. Trans. Am. Fish. Soc. 119, 673–688.

Coleman, F.C., Koenig, C.C., Collins, L.A., 1996. Reproductive styles of shallow-water groupers (Pisces: serranidae) in the eastern Gulf of Mexico and the consequences of fishing spawning aggregations. Environ. Biol. Fish. 47, 129–141.

Coleman, F.C., Koenig, C.C., Scanlon, K.M., Heppell, S., Heppell, S., Miller, M.W., 2010. Benthic habitat modification through excavation by red grouper, *Epinephelus morio*, in the northeastern Gulf of Mexico. Open Fish Sci. J. 3, 1–15.

Coleman, F.C., Scanlon, K.M., Koenig, C.C., 2011. Groupers on the edge: shelf edge spawning habitat in and around marine reserves of the northeastern Gulf of Mexico. Prof. Geogr. 63, 456–474.

Coleman, F.C., Williams, S.L., 2002. Overexploiting marine ecosystem engineers: potential consequences for biodiversity. Trends Ecol. Evol. 17, 40–44.

Colin, P.L., 2012. Aggregation spawning: biological aspects of the early life history. In: DeMitcheson, Y.S., Colin, P.L. (Eds.), Reef Fish Spawning Aggregations: Biology, Research and Management. Springer, Dordrecht, pp. 191–224.

Colin, P.L., Koenig, C.C., Laroche, W.A., 1996. Development from egg to juvenile of the red grouper (Epinephelus morio) (pisces: serranidae) in the laboratory. In: Arreguin-Sanchez, F., Munro, J.L., Balgos, M.C., Pauly, D. (Eds.), Biology, Fisheries and Culture of Tropical Groupers and Snappers: Proceedings of an EPOMEX/ICARM International Workshop on Tropical Snappers and Groupers. International Center for Living Aquatic Resources Management, University of Campeche, Mexico, pp. 399–414.

Collery, R.F., Veth, K.N., Dubis, A.M., Carroll, J., Link, B.A., 2014. Rapid, accurate, and non-invasive measurement of Zebrafish axial length and other eye dimensions using SD-OCT allows longitudinal analysis of myopia and emmetropization. PloS One 9.

Curtis, J.S., Albins, M.A., Peebles, E.B., Stallings, C.D., 2020. Stable isotope analysis of eye lenses from invasive lionfish yields record of resource use. Mar. Ecol. Prog. Ser. 637, 181–197.

Dalponti, G., Guariento, R.D., Caliman, A., 2018. Hunting high or low: body size drives trophic position among and within marine predators. Mar. Ecol. Prog. Ser. 597, 39–46.

Dorval, E., Jones, C.M., Hannigan, R., van Montfrans, J., 2007. Relating otolith chemistry to surface water chemistry in a coastal plain estuary. Can. J. Fish. Aquat. Sci. 64, 411–424.

Drass, D.M., Bootes, K.L., Lyczkowski-Shultz, J., Comyns, B.H., Holt, G.J., Riley, C.M., Phelps, R.P., 2000. Larval development of red snapper, *Lutjanus campechanus*, and comparisons with co-occurring snapper species. Fish. Bull. 98, 507–527.

Du, Q.S., Wei, D.Q., Chou, K.C., 2003. Correlations of amino acids in proteins. Peptides 24, 1863–1869.

Ellis, R.D., Powers, J.E., 2012. Gag Grouper, marine reserves, and density-dependent sex change in the Gulf of Mexico. Fish. Res. 115, 89–98.

Fitzhugh, G.R., Koenig, C.C., Coleman, F.C., Grimes, C.B., Sturges, W., 2005. Spatial and temporal patterns in fertilization and settlement of young gag (*Mycteroperca microlepis*) along the west Florida shelf. Bull. Mar. Sci. 77, 377–396.

Fry, B., Wainright, S.C., 1991. Diatom sources of C-13 rich carbon in marine food webs. Mar. Ecol. Prog. Ser. 76, 149–157.

Graham, B.S., Grubbs, D., Holland, K., Popp, B.N., 2007. A rapid ontogenetic shift in the diet of juvenile Yellowfin Tuna from Hawaii. Mar. Biol. 150, 647–658.

Graham, B.S., Koch, P.L., Newsome, S.D., McMahon, K.W., Aurioles, D., 2010. Using isoscapes to trace the movements and foraging behavior of top predators in oceanic ecosystems. In: West, J.B., Bowen, G.J., Dawson, T.E., Tu, K.P. (Eds.), Isoscapes: Understanding Movement, Pattern, and Process on Earth through Isotope Mapping, pp. 299–318.

Granneman, J.E., 2018. Evaluation of Trace-Metal and Isotopic Records as Techniques for Tracking Lifetime Movement Patterns in Fishes, College of Marine Science. University of South Florida, Tampa, FL, p. 144.

Grasty, S., Wall, C.C., Gray, J.W., Brizzolara, J., Murawski, S.A., 2019. Temporal persistence of Red Grouper holes and analysis of associated fish assemblages from towed camera data in the Steamboat Lumps marine protected area. Trans. Am. Fish. Soc. 1–9.

Guinan Jr., M.E., Kapuscinski, K.L., Teece, M.A., 2015. Seasonal diet shifts and trophic position of an invasive cyprinid, the Rudd *Scardinius erythrophthalmus* (Linnaeus, 1758), in the upper Niagara River. Aquat. Invasions 10, 217–225.

Haas, H.L., Freeman, C.J., Logan, J.M., Deegan, L., Gaines, E.F., 2009. Examining mummichog growth and movement: are some individuals making intra-season migrations to optimize growth? J. Exp. Mar. Biol. Ecol. 369, 8–16.

Hanson, N.N., Wurster, C.M., Eimf, Todd, C.D., 2013. Reconstructing marine life-history strategies of wild Atlantic salmon from the stable isotope composition of otoliths. Mar. Ecol. Prog. Ser. 475, 249–266.

Hine, A.C., Locker, S.D., 2011. The Florida Gulf of Mexico continental shelf—great contrasts and significant transitions. In: The Gulf of Mexico: Origin, Waters, and Marine Life.

Hollenbeck, C.M., Portnoy, D.S., Saillant, E., Gold, J.R., 2015. Population structure of red snapper (Lutjanus campechanus) in US waters of the western Atlantic Ocean and the northeastern Gulf of Mexico. Fish. Res. 172, 17–25.

Hood, P.B., Godcharles, M.F., Barco, R.S., 1994. Age, growth, reproduction, and the feeding ecology of black-sea bass, *Centropristis striata* (Pisces, Serranidae), in the eastern Gulf of Mexico. Bull. Mar. Sci. 54, 24–37.

Houde, E.D., 2009. Emerging from Hjort's shadow. J. Northwest Atl. Fish. Sci. 41, 53–70.

Huelster, S., 2015. Comparison of Isotope-Based Biomass Pathways with Groundfish Community Structure in the Eastern Gulf of Mexico, College of Marine Science. University of South Florida, Tampa, p. 161.

Jackson, A.L., Inger, R., Parnell, A.C., Bearhop, S., 2011. Comparing isotopic niche widths among and within communities: SIBER - stable Isotope Bayesian Ellipses in R. J. Anim. Ecol. 80, 595–602.

Johnson, A.G., Collins, L.A., 1994. Age-size structure of red grouper, (*Epinephelus morio*), from the eastern Gulf of Mexico. Northeast Gulf Sci. 13, 101–106.

Kimura, D.K., Lyons, J.J., 1991. Between-reader bias and variability in the age-determination process. Fish. Bull. 89, 53–60.

Kurth, B.N., Peebles, E., Stallings, C.D., 2019. Atlantic Tarpon (*Megalops atlanticus*) exhibit upper estuarine habitat dependence followed by foraging system fidelity after ontogenetic habitat shifts. Estuar. Coast Shelf Sci.

Lim, L.-S., Mukai, Y., 2014. Morphogenesis of sense organs and behavioural changes in larvae of the brown-marbled grouper *Epinephelus fuscoguttatus* (Forsskal). Mar. Freshw. Behav. Physiol. 47, 313–327.

Locker, S.D., Armstrong, R.A., Battista, T.A., Rooney, J.J., Sherman, C., Zawada, D.G., 2010. Geomorphology of mesophotic coral ecosystems: current perspectives on morphology, distribution, and mapping strategies. Coral Reefs 29, 329–345.

Lombardi-Carlson, L., 2014. Age and Growth Description of Red Grouper (*Epinephelus morio*) from the Northeastern Gulf of Mexico: 1978-2013, SEDAR 42 (North Charleston, SC).

Lorrain, A., Graham, B.S., Popp, B.N., Allain, V., Olson, R.J., Hunt, B.P.V., Potier, M., Fry, B., Galvan-Magana, F., Menkes, C.E.R., Kaehler, S., Menard, F., 2015. Nitrogen isotopic baselines and implications for estimating foraging habitat and trophic position of yellowfin tuna in the Indian and Pacific Oceans. Deep-Sea Res. Part II Top. Stud. Oceanogr. 113, 188–198.

Lynnerup, N., Kjeldsen, H., Heegaard, S., Jacobsen, C., Heinemeier, J., 2008. Radiocarbon dating of the human eye lens crystallines reveal proteins without carbon turnover throughout life. PloS One 3.

MacKenzie, K.M., Trueman, C.N., Palmer, M.R., Moore, A., Ibbotson, A.T., Beaumont, W. R.C., Davidson, I.C., 2012. Stable isotopes reveal age-dependent trophic level and spatial segregation during adult marine feeding in populations of salmon. ICES J. Mar. Sci. 69, 1637–1645.

Mahmoud, A., Sunarso, J., 2018. A new graphical method to target carbon dioxide emission reductions by simultaneously aligning fuel switching, energy saving, investment cost, carbon credit, and payback time. Int. J. Energy Res. 42, 1551–1562.

Mayer, D.A., Weisberg, R.H., Zheng, L.Y., Liu, Y.G., 2017. Winds on the West Florida Shelf: regional comparisons between observations and model estimates. Journal of Geophysical Research-Oceans 122, 834–846.

McMahon, K.W., Fogel, M.L., Johnson, B.J., Houghton, L.A., Thorrold, S.R., 2011. A new method to reconstruct fish diet and movement patterns from delta C-13 values in otolith amino acids. Can. J. Fish. Aquat. Sci. 68, 1330–1340.

McMahon, K.W., Hamady, L.L., Thorrold, S.R., 2013. A review of ecogeochemistry approaches to estimating movements of marine animals. Limnol. Oceanogr. 58, 697–714.

McMahon, K.W., McCarthy, M.D., 2016. Embracing variability in amino acid delta N-15 fractionation: mechanisms, implications, and applications for trophic ecology. Ecosphere 7.

McMeans, B.C., Kadoya, T., Pool, T.K., Holtgrieve, G.W., Lek, S., Kong, H., Winemiller, K., Elliot, V., Rooney, N., Laffaille, P., McCain, K.S., 2019. Consumer trophic positions respond variably to seasonally fluctuating environments. Ecology 1–10.

Meath, B., Peebles, E.B., Seibel, B.A., Judkins, H., 2019. Stable isotopes in the eye lenses of *Doryteuthis plei* (Blainville 1823): exploring natal origins and migratory patterns in the eastern Gulf of Mexico. Continent. Shelf Res.

Moe, M.A.J., 1969. Biology of the Red Grouper *Epinephelus morio* from the Eastern Gulf of Mexico. Florida Department of Natural Resources Marine Research Laboratory Professional Papers Series. Fish and Wildlife Research Institute, St. Petersburg, FL, pp. 1–95.

Mullaney, M.D., Gale, L.D., 1996. Ecomorphological relationships in ontogeny: anatomy and diet in gag, Mycteroperca microlepis (Pisces: serranidae), pp. 167–180. Copeia.

Nguyen, B.V.V., 2020. Investigation of Retention versus Export of Planktonic Fish Eggs in the Northeastern Gulf of Mexico, Marine Science. University of South Florida, Tampa, p. 97.

Nicol, J.A.C., 1989. The Eyes of Fishes. Clarendon, Oxford, England.

Nielsen, J., Hedeholm, R.B., Heinemeier, J., Bushnell, P.G., Christiansen, J.S., Ramsey, C. B., Brill, R.W., Simon, M., Steffensen, K.F., Steffensen, J.F., 2016. Eye lens radiocarbon reveals centuries of longevity in the Greenland shark (*Somniosus microcephalus*). Science 353, 702–704.

Nishida, K., Yasu, A., Nanjo, N., Takahashi, M., Kitajima, S., Ishimura, T., 2020. Microscale stable carbon and oxygen isotope measurement of individual otoliths of larvae and juveniles of Japanese anchovy and sardine. Estuar. Coast Shelf Sci.

Oksanen, J., Blanchet, F.G., Friendly, M., Kindt, R., Legendre, P., McGlinn, D., Minchin, P.R., O'Hara, R.B., Simpson, G.L., Solymos, P., Stevens, M.H.H., Szoecs, E., Wagner, H., 2019. Vegan: community ecology package. R package version 2.5-4.

Park, J.-M., Cho, J.-K., Han, K.-H., Kim, N.-r., Hwang, H.-K., Kim, K.-M., Myeong, J.-I., Son, M.-H., 2014. Early life history of the sevenband grouper, *Epinephelus septemfasciatus* from korea. Development and Reproduction 18, 13–23.

Peebles, E.B., Hollander, D.J., 2020. Combining isoscapes with tissue-specific isotope records to recreate the geographic histories of fish. In: Murawski, S.A., Ainsworth, C. H., Gilbert, S., Hollander, D.J., Paris, C.B., Schlüter, M., Wetzel, D.L. (Eds.),

Scenarios and Responses to Future Deep Oil Spills. Springer, Cham, Switzerland, pp. 203–218.
Post, D.M., 2002. Using stable isotopes to estimate trophic position: models, methods, and assumptions. Ecology 83, 703–718.
Powell, A.B., Tucker, J.W., 1992. Egg and larval development of laboratory-reared nassau grouper, Epinephelus striatus (pisces serranidae). Bull. Mar. Sci. 50, 171–185.
Quaeck-Davies, K., Bendall, V.A., MacKenzie, K.M., Hetherington, S., Newton, J., Trueman, C.N., 2018. Teleost and elasmobranch eye lenses as a target for life-history stable isotope analyses. PeerJ 6, 26.
R Core Team, 2019. R: A Language and Environment for Statistical Computing. R Foundation for Statistical Computing, Vienna, Austria. Version 3.6.1.
Radabaugh, K.R., Hollander, D.J., Peebles, E.B., 2013. Seasonal delta C-13 and delta N-15 isoscapes of fish populations along a continental shelf trophic gradient. Continent. Shelf Res. 68, 112–122.
Radabaugh, K.R., Malkin, E.M., Hollander, D.J., Peebles, E.B., 2014. Evidence for light-environment control of carbon isotope fractionation by benthic microalgal communities. Mar. Ecol. Prog. Ser. 495, 77–90.
Radabaugh, K.R., Peebles, E.B., 2014. Multiple regression models of $\delta^{13}C$ and $\delta^{15}N$ for fish populations in the eastern Gulf of Mexico. Continent. Shelf Res. 84, 158–168.
Roberts, D.E., Harpster, B.V., Havens, W., Halscott, K., 1976. Facilities and methodology for the culture of the southern Sea Bass (*Centropristis melana*). Jornal of the World Aquaculture Society 7, 163–198.
Salazar, G., 2019. EcolUtils: Utilities for Community Ecology Analysis. R package version 0.1.
Saul, S., Die, D., Brooks, E.N., Burns, K., 2012. An individual-based model of ontogenetic migration in reef fish using a biased random walk. Trans. Am. Fish. Soc. 141, 1439–1452.
Saul, S.E., Walter III, J.F., Die, D.J., Naarc, D.F., Donahue, B.T., 2013. Modeling the spatial distribution of commercially important reef fishes on the West Florida Shelf. Fish. Res. 143, 12–20.
Seminoff, J.A., Benson, S.R., Arthur, K.E., Eguchi, T., Dutton, P.H., Tapilatu, R.F., Popp, B.N., 2012. Stable isotope tracking of endangered sea turtles: validation with satellite telemetry and delta N-15 analysis of amino acids. PloS One 7.
Simpson, S., Sims, D., Trueman, C.N., 2019. Ontogenetic trends in resource partitioning and trophic geography of sympatric skates (Rajidae) inferred fromstable isotope composition across eye lenses. Mar. Ecol. Prog. Ser. 624, 103–116.
Sokal, R.R., Rohlf, F.J., 1994. Biometry: the Principles and Practices of Statistics in Biological Research Third, 3rd) edition.
Stallings, C.D., Coleman, F.C., Koenig, C.C., Markiewicz, D.A., 2010. Energy allocation in juveniles of a warm-temperate reef fish. Environ. Biol. Fish. 88, 389–398.
Stewart, D.N., Lango, J., Nambiar, K.P., Falso, M.J.S., FitzGerald, P.G., Rocke, D.M., Hammock, B.D., Buchholz, B.A., 2013. Carbon turnover in the water-soluble protein of the adult human lens. Mol. Vis. 19, 463–475.
Switzer, T.S., MacDonald, T.C., McMichael Jr., R.H., Keenan, S.F., 2012. Recruitment of juvenile Gags in the eastern Gulf of Mexico and factors contributing to observed spatial and temporal patterns of estuarine occupancy. Trans. Am. Fish. Soc. 141, 707–719.
Trueman, C.N., MacKenzie, K.M., Glew, K.S., 2017. Stable isotope-based location in a shelf sea setting: accuracy and precision are comparable to light-based location methods. Methods in Ecology and Evolution 8, 232–240.
Tzadik, O.E., Curtis, J.S., Granneman, J.E., Kurth, B.N., Pusack, T.J., Wallace, A.A., Hollander, D.J., Peebles, E.B., Stallings, C.D., 2017. Chemical archives in fishes beyond otoliths: a review on the use of other body parts as chronological recorders of microchemical constituents for expanding interpretations of environmental, ecological, and life-history changes. Limnol Oceanogr. Methods 15, 238–263.
Tzadik, O.E., Goddard, E.A., Hollander, D.J., Koenig, C.C., Stallings, C.D., 2015. Non-lethal approach identifies variability of delta N-15 values in the fin rays of Atlantic Goliath Grouper, Epinephelus itajara. Peerj 3.
Umezawa, Y., Tamaki, A., Suzuki, T., Takeuchi, S., Yoshimizu, C., Tayasu, I., 2018. Phytoplankton as a principal diet for callianassid shrimp larvae in coastal waters, estimated from laboratory rearing and stable isotope analysis. Mar. Ecol. Prog. Ser. 592, 141–158.
Vihtelic, T.S., 2008. Teleost lens development and degeneration. International Review of Cell and Molecular Biology 269 269, 341–373.
Wall, C.C., Donahue, B.T., Naar, D.F., Mann, D.A., 2011. Spatial and temporal variability of red grouper holes within steamboat lumps marine reserve, Gulf of Mexico. Mar. Ecol. Prog. Ser. 431, 243–254.
Wall, K.R., Stallings, C.D., 2018. Subtropical epibenthos varies with location, reef type, and grazing intensity. J. Exp. Mar. Biol. Ecol. 509, 54–65.
Wallace, A.A., Hollander, D.J., Peebles, E.B., 2014. Stable isotopes in fish eye lenses as potential recorders of trophic and geographic history. PloS One 9, e108935.
Weaver, D.C., 1996. Feeding Ecology and Ecomorphology of Three Seabasses (Pisces: Serranidae) in the Northeastern Gulf of Mexico. University of Florida, Gainesville, FL.
Weisberg, R.H., Zheng, L., Peebles, E.B., 2014. Gag grouper larvae pathways on the West Florida Shelf. Continent. Shelf Res. 88, 11–23.
Wells, R.J.D., Cowan, J.H., Fry, B., 2008. Feeding ecology of red snapper Lutjanus campechanus in the northern Gulf of Mexico. Mar. Ecol. Prog. Ser. 361, 213–225.
White, D.B., Palmer, S.M., 2004. Age, growth and redproduction of the red snapper, Lutjanus campechanus, from the southeastern U.S. Bull. Mar. Sci. 75, 335–360.
Zhang, J.Y., Fujiwara, A., Sawara, J., 2006. Multidimentional timing decisions: a case study in tourism behavior analysis. Tourism Anal. 11, 319–329.